Parametric Study of Multipath Propagation Effects on Terrestrial FSO Paths

Zdeněk Kolka[1], Viera Biolková[1] and Dalibor Biolek[2]
[1]Department of Radio Electronics, Brno University of Technology, Brno, Czech Republic
[2] Department of Electrical Engineering, University of Defence, Brno, Czech Republic
kolka@feec.vutbr.cz, biolkova@feec.vutbr.cz, dalibor.biolek@unob.cz

Abstract. Besides increased attenuation, scattering due to fog also imposes multiple propagation effects on Free-Space Optical links, which cause temporal broadening of transmitted pulses and intersymbol interference. The paper presents a parametric study, which evaluates the effects using a Monte-Carlo simulation based on the Mie scattering theory. All input parameters are clearly linked with FSO link design parameters. Simulation results are provided for typical continental fog parameters and a typical scenario for metro links.

Keywords: Free-space optical links, scattering, intersymbol interference, Monte Carlo simulation.

1 Introduction

Technology for gigabit Free-Space Optical (FSO) systems for metropolitan networks is now readily available on the market. The next technology step is characterized by data rates above 10 Gbs, which requires careful characterization of the atmospheric communication channel. The main atmospheric phenomena influencing optical links are scattering on water droplets of fog and atmospheric scintillation [1]-[3]. Short-haul metro FSO systems are designed with a sufficient link margin to accommodate attenuating effects of moderate fog, snow, and rain. Therefore the effect of atmospheric scintillation during clear-sky periods is not so significant. For lower data rates the atmospheric channel can be modeled as a simple channel with slowly-varying attenuation, which can reach hundreds of dB/km in fog [1], [2].

Besides increased attenuation, scattering due to fog also imposes multiple propagation paths, which causes temporal broadening of transmitted pulses, resulting in intersymbol interference (ISI).

The time-domain effects have been studied for ground-to-air or satellite communication through clouds [4], [5] mainly for military purposes, where the analyzed scenarios expected the utilization of multi-kilowatt pulses. Unfortunately, only few papers deal with an analysis of realistic scenarios for terrestrial FSO systems, where the transmitted power is limited by eye-safety regulation and affordable laser sources.

This paper deals with statistical simulation [6] of scattering on water droplets of fog implemented in MATLAB. Section 2 describes the simulation model used and Section 3 presents the parametric study for a realistic terrestrial FSO scenario.

2 Model of Multipath Propagation in Fog

2.1 Mie Scattering Theory

Light propagating through fog is scattered on water droplets. As the droplet diameter is comparable to wavelength, the process is described by the Mie theory. The type of fog is characterized by particle size distribution n (number of particles per unit volume per unit increment of radius), which is usually approximated by the modified gamma distribution [2]

$$n(r) = a\, r^{\alpha} e^{-b\, r} \ , \tag{1}$$

where r is the particle radius, and a, b, and α are coefficients, see Table 1. Radiation (continental) fog generally appears during the night and at the end of the day, particularly in valleys. Advection (maritime) fog is formed by the movement of wet and warm air masses above the colder maritime or terrestrial surfaces. The table gives typical values. However, actual fog parameters may vary significantly [2].

Table 1. Typical parameters of particle-size distribution [2].

Type of fog	*a*	*b*	α
Dense advection fog	0.027	0.3	3
Moderate advection fog	0.066	0.38	3
Dense radiation fog	2.37	1.5	6
Moderate radiation fog	607.5	3	6

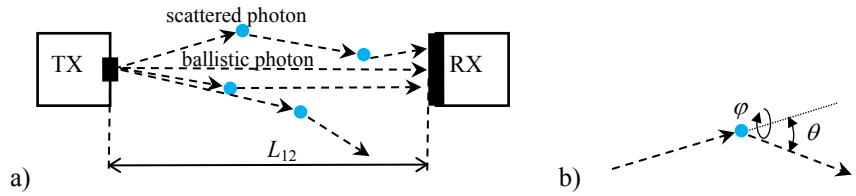

Fig. 1. a) Atmospheric optical channel with scattering; b) Geometry of scattering event.

The optical pulse can be regarded as a set of photons that interact with water droplets of fog, Fig. 1a. Each photon can be absorbed with probability P_{abs} or randomly "scattered". The fog density is characterized by the mean distance d_{av} between two interactions. The optical thickness of fog is then defined as

$$\tau = L_{12} / d_{av} \ . \tag{2}$$

The distance between two scatterings is an exponential random variable whose PDF and CDF are

$$f_d(d) = \exp(-d / d_{av}) \ / \ d_{av} \ , \quad F_d(d) = 1 - \exp(-d / d_{av}) \tag{3, 4}$$

The probability that a "ballistic" photon traveling along the optical axis reaches the receiver without being scattered is

$$P(d > L_{12}) = 1 - F_d(L_{12}) = \exp(-\tau) \ , \tag{5}$$

which gives the attenuation observed by a receiver with narrow field of view as

$$\alpha_s = 10\log(\exp\tau) = 4.34\,\tau \text{ [dB]} \ . \tag{6}$$

Formula (6) represents, in fact, the well-known Beer-Lambert law.

During interaction with a water droplet a photon is scattered at a random angle θ with arbitrary azimuthal rotation φ, Fig. 1b, [7]. The azimuth angle φ is uniformly distributed in $\langle 0, 2\pi)$. The PDF of scattering angle θ can be obtained from the Mie phase function $P(\theta)$ as

$$f_\theta(\theta) = P(\theta)\sin(\theta)/2 \ . \tag{7}$$

The phase function depends on the wavelength and spectrum of droplet diameters (see Table I). It can be obtained together with P_{abs} using the *BHMIE* [7] algorithm, which is implemented in the *MiePlot* software [8]. Figure 2 shows the cumulative distribution function of (7) for fog parameters from Tab. I.

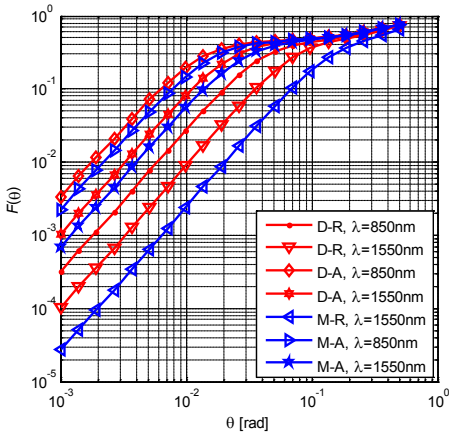

Fig. 2. Cumulative distribution function of (7) for different parameters of fog (D – dense, M – moderate, A – advection, R – radiation).

2.2 Monte-Carlo Simulation

As there is no closed solution for light propagating in scattering media the results should be obtained by tracing each random "photon" from a sufficiently large set.

Let **v** be a vector and **k** a unit vector describing an axis of rotation about which we want to rotate **v** by an angle ϕ, then the rotated vector $\mathbf{v}_{rot}$ will be [9]

$$\mathbf{v}_{rot} = R(\mathbf{v}, \mathbf{k}, \phi) = \mathbf{v}\cos\phi + (\mathbf{k}\times\mathbf{v})\sin\phi + \mathbf{k}(\mathbf{k}\cdot\mathbf{v})(1-\cos\phi) \ . \tag{8}$$

Each photon is represented by its position **p**, the velocity direction vector **v**, and the normal vector **n**. Both **v** and **n** are the unit vectors. The simulation algorithm, which is applied to each photon, is as follows:

1. Generate initial vectors $\mathbf{v}_0$, $\mathbf{p}_0$, and $\mathbf{n}_0$.
2. Generate random distance d to the next collision using exponential PDF (3). Update position **p** as follows

$$\mathbf{p}_{i+1} = \mathbf{p}_i + d\,\mathbf{v}_i\,. \tag{9}$$

3. Delete photons whose position is too far from the beam center from further simulation. Compute and save exact time of arrival for photons that reach the receiving aperture within the field of view.
4. Delete photons that will be absorbed. Generate random rotation φ with uniform PDF on $\langle 0, 2\pi)$ and deflection θ with PDF (7). Modify vectors **v** and **n** of remaining photons using (8) as follows

$$\mathbf{n}_{i+1} = R(\mathbf{n}_i\,,\,\mathbf{v}_i,\,\varphi)\,,\ \mathbf{v}_{i+1} = R(\mathbf{v}_i\,,\,\mathbf{n}_{i+1},\,\theta) \tag{10, 11}$$

5. Repeat steps 2 to 4 until no photon remains.

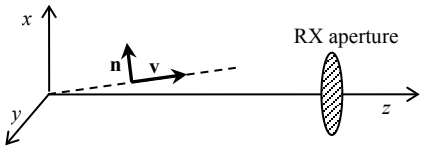

Fig. 3. Coordinate system for Monte-Carlo simulation.

2.2 Impulse Response Approximation

The result of the Monte-Carlo algorithm is a set of arrival times of photons that reached the RX aperture. As all photons are "transmitted" at the same time the probability density function of arrival times represents the impulse response of the channel, which can be approximated by the double gamma function [6]

$$h(t) = k_0\delta(t) + k_1 t\exp(-k_2 t) + k_3 t\exp(-k_4 t) \quad \text{for } t \geq 0\,, \tag{12}$$

where the Dirac pulse $k_0\delta(t)$ represents the ballistic photons arriving at the same time. Coefficients k_1 to k_4 define the fast and the slow delayed responses and can be obtained by curve fitting. The time origin of (12) corresponds to the propagation delay along the line of sight, i.e. L_{12}/c. In the frequency domain the response is

$$H(j\omega) = k_0 + \frac{k_1/k_2^2}{(1+j\omega/k_2)^2} + \frac{k_3/k_4^2}{(1+j\omega/k_4)^2} = k_0\left[1 + \frac{k_{d1}}{(1+j\omega/k_2)^2} + \frac{k_{d2}}{(1+j\omega/k_4)^2}\right]. \tag{13}$$

3 Simulation Results

Let us consider a typical metro FSO system with receiving aperture $D_{\mathrm{RXA}} = 0.2$ m installed on path $L_{12} = 1000$ m.

Fig. 4 shows the dependence of the attenuation for ballistic and delayed photons on the attenuation α_s (6), which can be represented by photon numbers as

$$\alpha_{ball} = 10\log\left(N_{ball}/N_{RX}\right),\ \alpha_{delay} = 10\log\left(N_{delay}/N_{RX}\right)\,, \tag{14}$$

where N_{ball} and N_{delay} are the number of ballistic and delayed photons, respectively ($N_{RX} = N_{ball} + N_{delay}$). The receiver acceptance half-angle $\theta_{RX} = 20$ mrad and the beam divergence half-angle θ_{TX} is 1 mrad or 2 mrad. The presented attenuation includes the

free-space path loss. As can be seen the energy of delayed photons is greater than the energy of ballistic photons for $\alpha_s > 35$ dB and $\theta_{TX} = 2$ mrad.

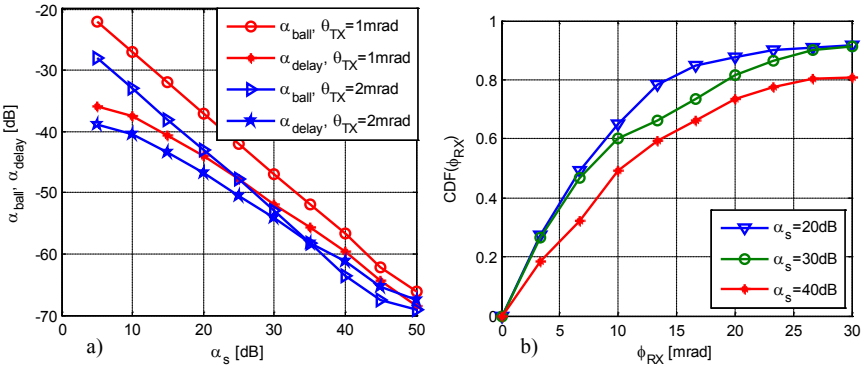

Fig. 4. a) Attenuation for ballistic and delayed photons ($\theta_{RX} = 20$ mrad); b) Cumulative distribution function of angle of incidence of photons on the receiving aperture.

Fig. 4b shows the cumulative distribution function of angle of incidence of photons on the receiving aperture. As the receiver acceptance half-angle θ_{RX} below 5 mrad is impractical the possibilities of filtering-out the delayed photons using narrow field of view are limited. The practical suppression would be in the order of 50%, i.e. 3dB.

Table 2. Identified parameters of channel response (13).

α_s [dB]	k_0	k_{d1}	k_{d2}	f_{d1} [GHz]	f_{d2} [GHz]
5	$1{,}6\cdot10^{-3}$	0,029	0,046	81	19,2
15	$1{,}6\cdot10^{-4}$	0,091	0,162	82	16,9
20	$5{,}0\cdot10^{-5}$	0,134	0,242	80	16,6
25	$1{,}5\cdot10^{-5}$	0,166	0,338	80	15,5
30	$4{,}8\cdot10^{-6}$	0,216	0,493	82	15,2
35	$1{,}4\cdot10^{-6}$	0,300	0,712	109	13,3
40	$4{,}3\cdot10^{-7}$	0,225	0,969	103	14,8

Tab. 2 shows parameters of channel frequency response (14) for $\theta_{RX} = 20$ mrad and $\theta_{TX} = 2$ mrad for different values of α_s based on simulation of 10^8 photons. Coefficients k_{d1} and k_{d2} represent the amplitude of fast and slow delayed responses relatively to ballistic photons. For large attenuations the set of received photons is small, which decreases the confidentiality of identified parameters.

As can be seen the delayed response becomes significant for α_s above 25 dB. The 3dB-bandwidth of both responses is shown in last two columns. Bandwidth of the slow response is only 15 GHz.

4 Conclusions

The paper describes in detail an implementation of the Monte-Carlo method for simulation of the multipath propagation of laser pulse in fog. Numerical results for a typical metropolitan link show the channel bandwidth during fog is in the order of tens of GHz. The amplitude of delayed response becomes significant for atmospheric attenuation above 25 dB.

Acknowledgement
This work has been supported by the Czech Science Foundation under grant No. P102/11/1376, by the Czech Ministry of Industry and Trade under grant agreement No.FR-TI4/148, and by and the Project for the development of K217 Department, UD Brno. The described research was performed in laboratories supported by the SIX project, registration number CZ.1.05/2.1.00/03.0072, operational programme Research and Development for Innovation.

References

[1] F. Nadeem, V. Kvicera, M. S. Awan, E. Leitgeb, S. S. Muhammad, G. Kandus, Weather Effects on Hybrid FSO/RF Communication Link. *IEEE J. Sel. Areas in Comm.*, vol.27, no.9, Dec. 2009, pp. 1687-1697.
[2] M.S. Awan, E. Leitgeb, S.S. Muhammad, Marzuki, F. Nadeem, M.S. Khan, C. Capsoni, Distribution Function for Continental and Maritime Fog Environments for Optical Wireless Communication. In *Proc. of the 6th Symposium on Communication Systems, Networks and Digital Signal Processing*, 2008, Graz, Austria, pp. 260 – 264.
[3] D. Giggenbach, H. Henniger, Fading-loss assessment in atmospheric freespace optical communication links with on-off keying. *Opt. Eng.*, vol. 47, April 2008, pp. 046001
[4] E. A. Bucher, R. M. Lerner, Experiments on Light Pulse Communication and Propagation through Atmospheric Thick Clouds. *Appl. Opt.* vol. 12, no. 10, pp 2401-2414, 1973.
[5] S. Arnon, D. Sadot, and N. S. Kopeika, Simple mathematical models for temporal, spatial, angular characteristics of light propagating through the atmosphere for space optical communication: Monte Carlo simulations. *J. Mod. Opt.*, Vol. 41, pp. 1955-1972, 1994.
[6] S. Lee, M. Kavehrad, Airborne Laser Communications with Impulse Response Shortening and Viterbi decoding. In *Proc of IEEE Military Communications Conference*, 2006.
[7] C. F. Bohren and D. R. Huffman, *Absorption and Scattering of Light by Small Particles*, John Wiley and Sons, New York, 1983.
[8] http://www.philiplaven.com
[9] G. Taubin, 3D Rotations. *IEEE Computer Graphics and Applications*, vol.31, no.6, pp.84,89, Nov.-Dec. 2011.